Regular Article

Effect of Powdered Cellulose Nanofiber with Different Particle Sizes on the Physical Properties of Tablets Manufactured *via* Direct Compression

Shohei Nakamura, Mai Jinno, Momoka Hamaoka, Ayumi Sakurada, and Takatoshi Sakamoto*

Department of Pharmaceutical Technology, School of Clinical Pharmacy, College of Pharmaceutical Sciences, Matsuyama University, 4–2 Bunkyo-cho, Matsuyama, Ehime 790–8578, Japan.
Received August 29, 2023; accepted October 4, 2023

Direct compression is a tableting technique that involves a few steps in non-demanding manufacturing conditions. High strength and rapid disintegration of tablet formulations were previously achieved through the addition of cellulose nanofibers (CNFs), which have recently attracted attention as a high-performance biomass material. However, CNF addition results in greater variation in tablet weight and drug content, potentially due to differences in particle size between CNF and other additives. Herein, we used pulverized CNF to evaluate the effect of CNF particle size on the variation in tablet weight and drug content. Tablet formulations consisted of CNF with different particle sizes (approximately 100 μm [CNF_{100}] and 300 μm [CNF_{300}], at 0, 10, 30, or 50%), lactose hydrate, acetaminophen, and magnesium stearate. Ten powder formulations with different particle sizes and CNF concentrations were prepared; thereafter, the tablets were produced using a rotary tableting press with a compression force of 10 kN. The variation in weight and drug content as well as the tensile strength, friability, disintegration time, and drug dissolution of tablets were evaluated. CNF_{100} addition to the tablets reduced the weight and drug content variation to a greater extent than CNF_{300} addition. Using CNF_{300}, we produced tablets of sufficient strength and short disintegration time. These properties were also achieved with CNF_{100} addition. Our findings suggest that adding CNF of small particle size to the tablet formulation can reduce the variation in weight and drug content while maintaining high strength and short disintegration time.

Key words cellulose nanofiber, powder characteristic, tablet property, direct compression, multifunctional additive

Introduction

Tablets are a convenient dosage form for patients as they are easy to carry and store, in addition to their accurate dosage. By coating the tablet, it is possible to mask the bitterness of the active ingredient and add various functionalities, such as sustained release, limited-time, and enteric coating.[1] To produce tablets that meet clinical and market demands, pharmaceutical companies use high-speed tablet presses. Robust tablet quality should therefore be ensured and adapted to the various manufacturing environments.[2–4]

The well-established technique of wet granule compression enables considerable tablet robustness.[5–7] In recent years, direct compression, which requires fewer steps, has attracted increasing attention.[8] In addition to the fewer steps required relative to wet granule compression, this technique can be performed in less-demanding manufacturing conditions. The reduced equipment, energy, and operating time required for the granulation process achieve a great reduction in cost and greater production efficiency. Therefore, direct compression has been the first choice for tablet manufacture in the United States in recent years.[9] However, because the formulation powder, which is simply a mixture of the active ingredient and excipients, is placed into the tableting press and continuously compressed at a high speed, the weight and drug content of tablets tend to fluctuate greatly. To address these problems, in addition to examining formulation and manufacturing conditions, extensive research has focused on improving equipment and developing new additives.[10–17]

In recent years, cellulose nanofibers (CNFs), which are made by refining cellulose, the main component of plant cell walls, have attracted attention in various fields as a high-performance biomass material.[18] In Japan, the Ministry of the Environment is promoting a CNF performance evaluation model project aimed at reducing CO_2 emissions, and naturally-derived CNFs extracted from plants are expected to contribute to the realization of a low-carbon society.[19] Various companies and research institutes are currently participating in this project, with rigorous competition in development.

CNFs possess a large specific surface area owing to their fine fiber structure, in addition to remarkable properties, such as high strength, elasticity, and viscosity, while also being light in weight. Further, CNFs offer the advantage of being a renewable resource, with favorable characteristics such as biodegradability and biocompatibility. In the medical field, research on CNFs is underway for applications, such as wound treatment, scaffolding materials for bone grafting, artificial organs, and functional contact lenses.[20,21] In the pharmaceutical industry, CNFs hold potential for improving drug delivery, release, and solubility, owing to their enormous specific surface area.[22–28]

In direct compression, it is essential to increase the binding force between powder particles to form a tablet of sufficient strength. Therefore, microcrystalline cellulose (MCC), which is easily plastically deformed, has conventionally been used as a dry binder. Furthermore, disintegration of a tablet in water, which has a trade-off relationship with binding properties, affects not only the absorption and bioavailability of the drug, but also other characteristics of the formulation, such as rapid

* To whom correspondence should be addressed. e-mail: sakamoto@g.matsuyama-u.ac.jp

dissolution. To achieve the required disintegration characteristics, disintegrants with different disintegration capacities are selected separately from the binder and are added in combination in an optimal ratio. However, their inclusion as separate additives results in them constituting a certain proportion of the formulation. When a single additive can achieve both binding and disintegrating properties, it is not only advantageous when considering additive selection in formulation design, but also in determining the quality of the final product. Further, this approach is not complicated. Therefore, CNF, which increases the strength and disintegration of tablets to which it is added, is promising as a multifunctional additive with multiple functions. Previous studies have evaluated CNF as a novel additive with both binding and disintegrating functions.[29,30] However, given the novelty of CNFs as materials and their limited exploration of applicability as pharmaceutical excipients, a comprehensive assessment of the effects of incorporating CNFs into the tablet formulation powder on the final product has been lacking.

In the present study, we focused on the strength and disintegration properties of CNF, evaluated the effect of CNF particle size on the physical properties of tablets manufactured *via* direct compression, and investigated the effectiveness of CNF as a multifunctional additive.

Results and Discussion

Comparison of CNF with Other Common Additives Commonly used additives, including MCC, low-substituted hydroxypropyl cellulose (L-HPC), crospovidone (CP), and croscarmellose sodium (CCS), were added to prepare tablets under the same manufacturing conditions for comparison with CNF. Figure 1 shows the relationship between tensile strength and disintegration time of the model tablets including each additive. The tablets to which MCC was added exhibited sufficient strength, with a tensile strength of 1.9 MPa. However, these tablets took longer to disintegrate (269 s) than the rest of the other tablets. The disintegration times of tablets containing L-HPC, CP, and CCS were within 60 s, showing sufficient disintegration ability. However, their tensile strengths were between 0.7–0.9 MPa, which was insufficient to maintain tablet shape. On the other hand, the model tablets to which CNF_{100} or CNF_{300} were added exhibited tensile strengths of 1.3 and 1.6 MPa, respectively, which was strong enough to withstand normal handling. Moreover, the disintegration times these tablets were 145 and 35 s, respectively, which was sufficiently short. The tablets containing CNF_{100} or CNF_{300} had tensile strengths ≥1 MPa and disintegration times ≤180 s. These results show that addition of CNF imparts sufficient tablet strength for adequate product handling and imparts a short disintegration time. Thus, we suggest that CNF can be used as an additive that satisfies both the tensile strength and disintegration standards for tablets manufactured *via* direct compression.

Physical Properties of CNF Raw Powder Untreated CNF_{300} and pulverized CNF_{100} particles were observed using scanning electron microscopy (SEM). Figure 2 shows the particle shapes and surface conditions of each CNF sample. CNF_{300} particles were composed of irregular tabular grains with sharp contours (Fig. 2b). By contrast, CNF_{100} particles were rounded, with the corners of the particle outlines scraped off owing to abrasion during pulverization (Fig. 2a). When the surfaces of these particles were observed at high magnification, they were all uneven, with undulations and depressions. Field emission scanning electron microscopy (FE-SEM) observation of the structure of CNF particles revealed an entanglement of fibers with a thickness of 50–100 nm (Fig. 2c). It is speculated that this nanosized fibrous structure contributed to the characteristic properties of each CNF, as described in the following paragraph.

Table 1 lists the physical properties of raw CNF powders. The untreated raw material, CNF_{300}, had an average particle

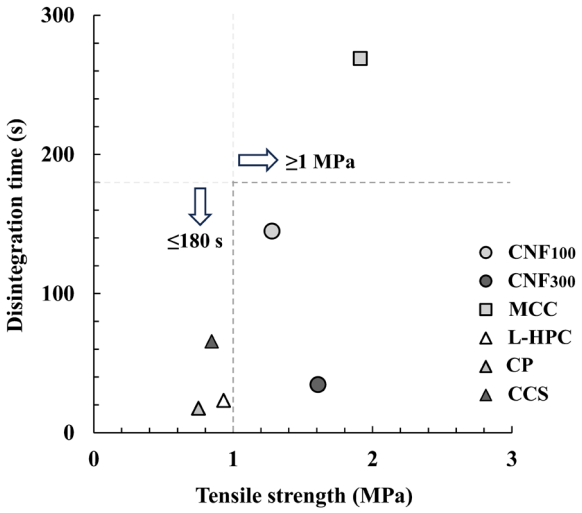

Fig. 1. Relationship between Tensile Strength and Disintegration Time of the Model Tablets Including CNF and Common Additives

CNF, cellulose nanofiber; MCC, microcrystalline cellulose; L-HPC, low-substituted hydroxypropyl cellulose; CP, crospovidone; CCS, croscarmellose sodium.

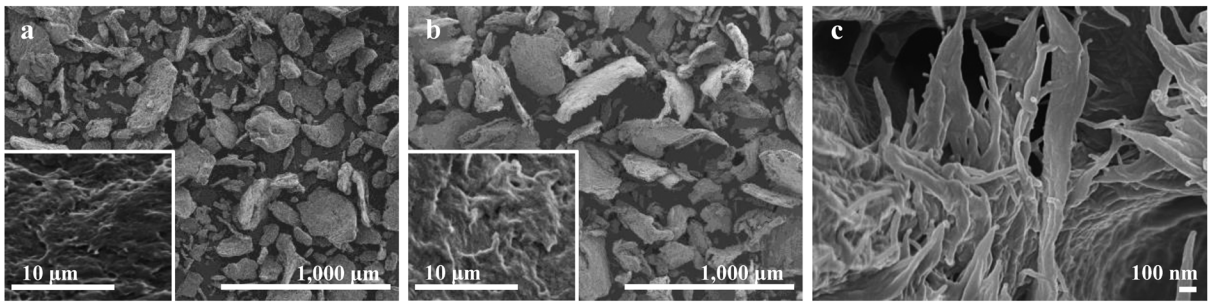

Fig. 2. Particle Shape and Surface Conditions of Each CNF

(a) CNF_{100} observed *via* SEM, (b) CNF_{300} observed *via* SEM, (c) nanofiber structure of the CNF particles observed *via* FE-SEM. The insets in a and b show the surface conditions observed at high magnification. CNF, cellulose nanofiber; SEM, scanning electron microscopy; FE-SEM, Field emission scanning electron microscopy.

Table 1. Physical Properties of CNF Raw Powder

	CNF_{100}	CNF_{300}
Average particle size (μm)	104.28 ± 2.00	290.75 ± 13.03
Geometric standard deviation	1.89 ± 0.04	1.60 ± 0.07
True density (g/mL)	1.502 ± 0.001	1.536 ± 0.024
Tap density (g/mL)	0.796 ± 0.001	0.365 ± 0.001
Bulk density (g/mL)	0.570 ± 0.004	0.263 ± 0.002
AOR (deg.)	51.1 ± 0.75	49.7 ± 0.30
AIF (deg.)	11.22 ± 2.16	11.46 ± 1.40
Contact angle (deg.)	87.56 ± 0.47	73.84 ± 1.02
Permeation rate (g^2/s)	0.058 ± 0.016	0.749 ± 0.032
Water retention (w/w %)	68.74 ± 2.99	68.31 ± 0.87

CNF, cellulose nanofiber; AOR, angle of repose; AIF, angle of internal friction.

size of 290.75 ± 13.03 μm, which was greater than that of other additives in the formulation. By contrast, the average particle size of CNF_{100} was 104.28 ± 2.00 μm, and it was possible to prepare CNF powder with a small particle size by pulverizing CNF_{300}. The geometric standard deviation, which represents particle size distribution, was slightly larger for CNF_{100}. This is attributed to the fine powder generated during pulverization. The true densities of both CNFs were similar, but the tapped and bulk densities of CNF_{100} were higher than those of CNF_{300}. This indicated that the pulverized CNF_{100} was packed more densely by tapping, and the voids in the powder bed were smaller. In addition, CNF_{100} had a slightly larger angle of repose (AOR). However, according to Carr's flowability index, both were powders with "poor flowability."[31] Almost identical values were noted for the angle of internal friction (AIF), which expresses flowability or friction under load. Contact angles obtained from Washburn's equation showed that both CNFs undergo immersion wetting. Further, the amount of liquid permeated into the powder bed 60 s after water absorption was 1.85 ± 0.25 mL for CNF_{100} and 6.70 ± 0.14 mL for CNF_{300}. The obtained permeation rate for CNF_{300} was ≥10 times higher than that of CNF_{100}, indicating that water permeated much faster in CNF_{300} than in CNF_{100}. The water retention capacity of the water-soaked CNF was approximately 68%, attributable to voids within the particles. This property enables the CNFs to retain a quantity of water equivalent to twice its own weight. This was speculated to be a consequence of the voids formed by nanosized fibers not being blocked even after pulverization, with a large amount of water retained in the voids within particles, regardless of particle size.

Figure 3 shows the powder X-ray diffraction spectra of CNF_{100}, CNF_{300}, and MCC as reference materials. The spectrum of each CNF was the same as that of MCC, indicating that pulverization of CNF did not affect its crystal structure.

Physical Properties of CNF-Containing Tablets To evaluate the effect of CNF particle size on the physical properties of tablets, the latter were manufactured using a compression force of 10 kN. The variations in weight, drug content as well as tensile strength, friability, disintegration time, and drug dissolution were then evaluated.

Weight Variation of Tablets

Figure 4a shows the weight variation in tablets to which CNF had been added. When ≥30% CNF_{300} was added, the weight variation was ≥1%, complicating the manufacture of tablets with a stable weight. However, when pulverized CNF_{100} at ≤50% was used, the variation in weight was

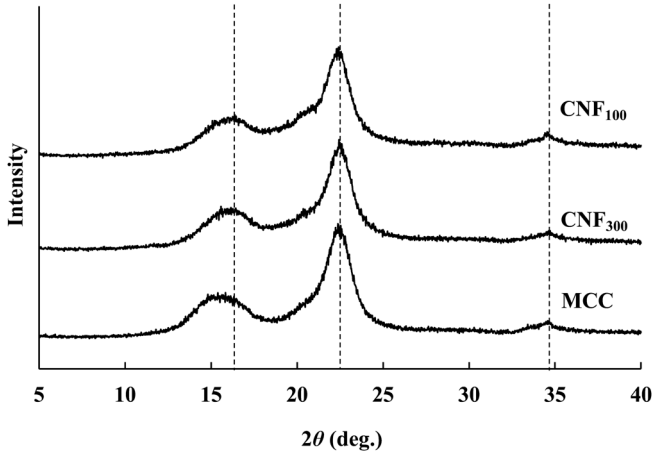

Fig. 3. Comparison of CNF Crystallinity

CNF, cellulose nanofiber; MCC, microcrystalline cellulose.

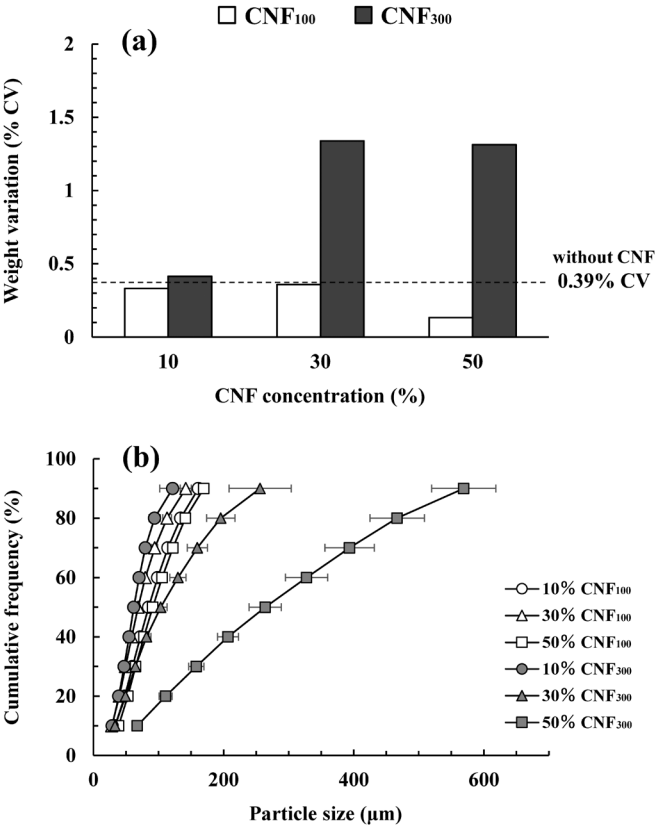

Fig. 4. Relationship between Particle Size Distribution of Formulation Powder with Added CNF and Weight Variation in Tablets

(a) Weight variation in tablets, (b) cumulative frequency of formulation powder particle size. CNF, cellulose nanofiber.

≤0.5%, allowing for the production of tablets with a stable weight. Typically, smaller particle sizes of the powder correspond to diminished flowability and increased weight variation during tablet manufacture. However, for tablets produced in this study, CNF_{100} addition resulted in smaller weight variation than CNF_{300} addition at all amounts tested. We therefore speculated that this result was not due to powder flowability. Thus, following the addition of 30–50% CNF_{300}, the particle size was distributed over a wide range (Fig. 4b). It was speculated that the observed variation reflected the non-uniform

filling of the formulation powder into the die during tableting. In the case of CNF_{100}, even when added at 50%, a narrow particle size distribution was observed, and we presumed that the formulation powder could be accurately scraped off during tablet manufacture.

Drug Content Variation in Tablets

Figure 5a shows the variation in drug content for each CNF-containing tablet. In the case of CNF_{300}, the drug content variation was approximately 2% for all added amounts, and the formulation with ≥30% added slightly exceeded 2%. By contrast, when CNF_{100} was added, the variation in drug content was smaller than that for CNF_{300} at any added amount, and the uniformity of the active ingredient in the formulation was improved. Further, when the acceptance value for each formulation was calculated, all tablets were ≤15%, and we were able to manufacture tablets that conformed to the uniformity of dosage units in the 18th Japanese Pharmacopoeia (Fig. 5b). In previous studies,[32,33] it was shown that the dispersion of a drug in the formulation powder was highly correlated with the AIF of the formulation powder. The larger AIF, the more the drug adhered to excipients and showed higher dispersibility. This is thought to be due to electrostatic adhesion between the drug and other additives. Therefore, we believe that the evaluation of drug content uniformity based on the AIF is an index that can be established between the drug and excipient under limited conditions for each formulation. Under these limited conditions, a linear relationship is observed between the AIF and drug content variation, making it possible to estimate drug content uniformity. We analyzed the variation relationship and evaluated the dispersion of each CNF in the formulation powder. Figure 5c shows the relationship between the AIF and drug content variation. A high negative correlation was observed (coefficient of determination $[R^2] = 0.5856$). Further, CNF_{100}, whose addition resulted in a lower drug content variation, had a higher AIF than CNF_{300}. CNF_{100} was uniformly dispersed in the formulation powder, and segregation of the drug was therefore less likely to occur.

Tensile Strength and Friability of Tablets

Figure 6 shows the tensile strength and friability of each CNF-containing tablet. When CNF_{300} was added at 50%, the tensile strength increased slightly, while no change in tensile strength was observed at lower added amounts (Fig. 6a). In the case of CNF_{100}, no amount of it had an effect on tensile strength. All of the tablets examined in this study exhibited a tensile strength of ≥1 MPa and could therefore satisfy the minimum hardness of 30 N required for general products.

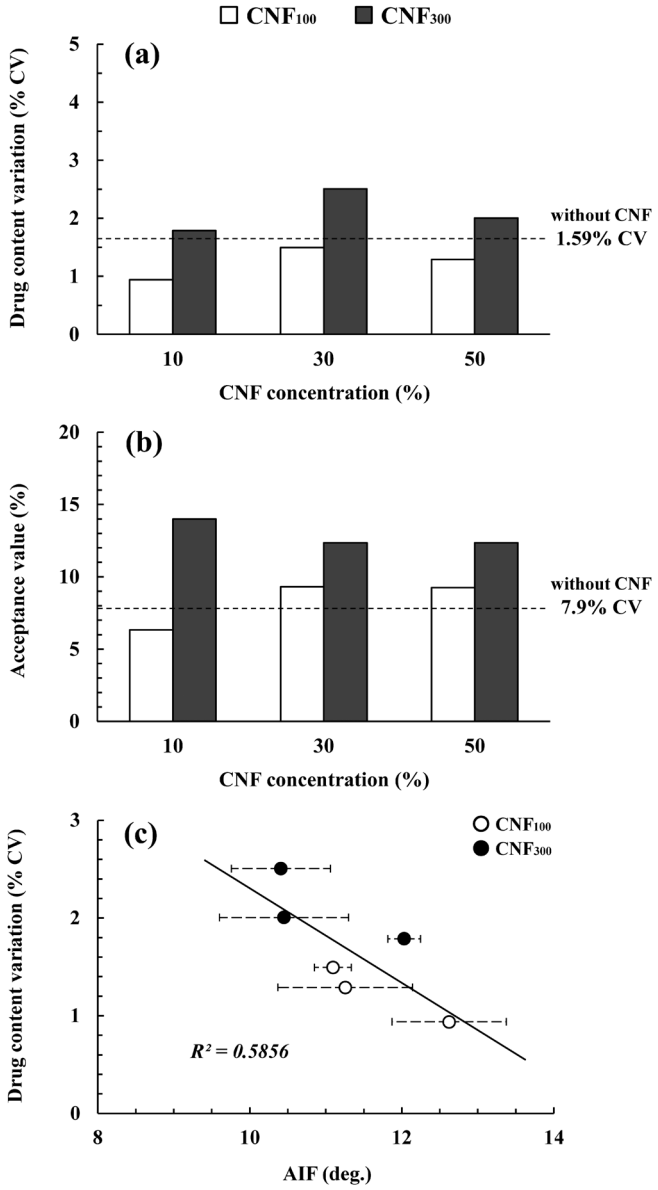

Fig. 5. Relationship between the AIF of CNF-Containing Formulation Powder and Tablet Drug Content Variation

(a) Drug content variation, (b) acceptance value, (c) relationships between the AIF of the formulation powder and drug content variation. CNF, cellulose nanofiber; AIF, angle of internal friction; R^2, coefficient of determination.

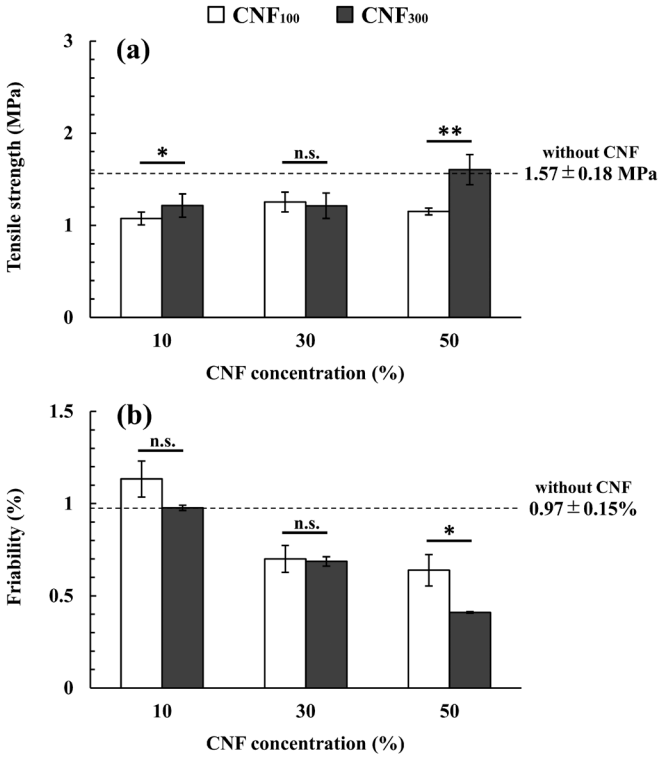

Fig. 6. Tensile Strength and Friability of CNF-Containing Tablets

(a) Tensile strength ($n = 10$), (b) friability ($n = 3$). The compression force during manufacture of each tablet was 10 kN. Data are presented as the mean ± standard deviation (S.D.). Differences between tablets prepared using different additives were assessed *via* the Student's *t*-test or the Mann–Whitney *U* test; $^{**}p < 0.001$, $^{*}p < 0.05$, n.s., not significant. CNF, cellulose nanofiber.

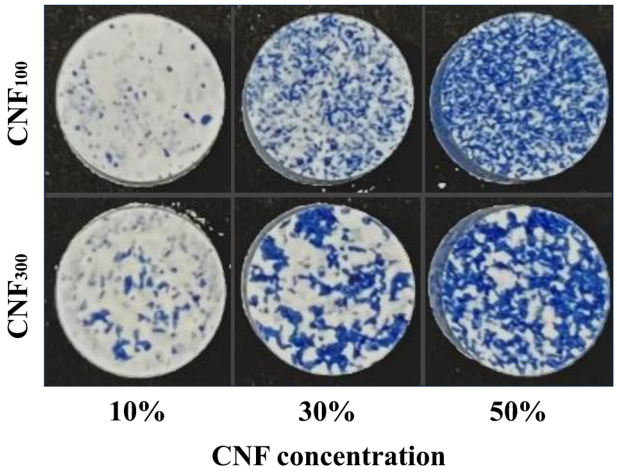

Fig. 7. Flat Surface of Tablets Manufactured Using Colored CNF

CNF, cellulose nanofiber.

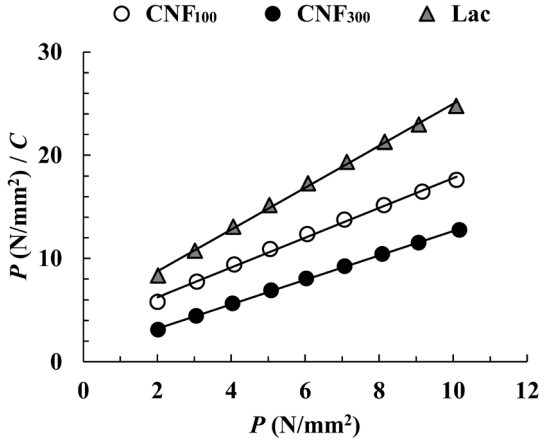

Fig. 8. Relationship between Vertical Load (P) and P/Compressed Volume (C) for Powder Bed Consisting of Pure CNF and Lac Powder

P, vertical load; C, volume reduction; CNF, cellulose nanofiber; Lac, lactose hydrate.

Table 2. Percentage of CNF-Occupied Area on the Tablet Surface

	10% addition	30% addition	50% addition
CNF_{100}	6.20 ± 2.41%	25.16 ± 5.11%	44.99 ± 4.25%
CNF_{300}	13.72 ± 3.40%	34.77 ± 4.50%	55.36 ± 4.75%

CNF, cellulose nanofiber.

Table 3. Characteristic Constants a and $1/b$ Obtained from Kawakita's Equation

	a	$1/b$
CNF_{100}	0.690	2.303
CNF_{300}	0.843	0.699
Lac	0.479	2.035

a, initial porosity; b, characteristic constants of the powder; CNF, cellulose nanofiber; Lac, lactose hydrate.

When the amount of CNF added was ≤30%, an effect of CNF particle size on tensile strength was not observed. It is considered that all CNF particles were plastically deformed by the compression force applied during tableting and were widely dispersed within the tablet, increasing its strength. At that point, CNF_{300}, which had a large particle size, was considered to show a behavior similar to that of CNF_{100}, as both particles were destroyed by compression.

Figure 6b shows the friability of each CNF-containing tablet. Regardless of the amount of CNF added, the friability of CNF_{100} was lower than that of CNF_{300}. Friability decreased with an increase in CNF content. The friability of tablets produced with a compression force of 10 kN was ≤1% when CNFs were added at ≥30%. In particular, since a large amount of CNF was present on the surface of the tablet containing 50% CNF, it was assumed that CNF_{300} particles were plastically deformed by compression, forming a more robust tablet than in the case of CNF_{100}. Therefore, to confirm the presence of CNF on the tablet surface, the surface of tablets produced using dye-colored CNF was observed under a microscope. Figure 7 shows an image of the flat surface of the tablet. In addition, Table 2 shows the percentage of the colored area (*i.e.*, the area where CNF exist) on the flat surface of each tablet. CNF_{100} was uniformly dispersed over the entire flat surface at all added amounts, but CNF_{300} had an uneven distribution, and portions without CNF were also observed. The CNF_{100} formulation demonstrated slightly lower values of the CNF-occupied area on the tablet surface in comparison to the CNF_{300} composition for any given quantity added (Table 2). It was assumed that a portion of the material did not appear on the surface. In the case of CNF_{300}, the value was slightly larger than the composition of CNF for any amount added. This was probably because the CNFs with a large particle size present on the tablet surface were deformed into a flat state by compression, thus covering other additives.

A compression test was performed on a powder bed composed of CNF and Lac raw powder to evaluate the differences in compression properties between the granules used in this study. Figure 8 shows compression test results for each CNF and Lac to Eq. 2. Both CNF and Lac fit Kawakita's equation, and a linear relationship was established between P and P/C (CNF_{100}, $R^2 = 0.9958$; CNF_{300}, $R^2 = 0.9995$; Lac, $R^2 = 0.9977$). When evaluating powder bed characteristics, the constants a and $1/b$ are considered. Their values obtained from the regression line shown in Fig. 8 are listed in Table 3. Generally, the larger the value of a, the more significant the bulk volume change during compression. Based on the value of a for each CNF, it was inferred that CNF_{300} caused the greatest particle deformation owing to the compression force during tableting, thus forming tablets with high density. Alternatively, the larger the value of $1/b$, the larger the yield stress as well as particle strength, and the lower the compactibility. The $1/b$ values were in the order of $CNF_{100} > Lac > CNF_{300}$, indicating that deformation due to the compression of CNF_{100} is unlikely to occur. These results suggest that the bulky CNF_{300} deformed the most during compression and formed tablets of high strength. By contrast, no considerable particle deformation was observed for CNF_{100}, even when compressed, suggesting that tablets with relatively large interparticle voids were obtained compared with that for CNF_{300}.

Figure 9 shows the roughness of the flat surface of each tablet. The surface roughness of CNF_{300}, which has a larger particle size, was lower than that of CNF_{100} at all added amounts. It was suggested that CNF_{100} was difficult to deform owing to its small particle size, whereas CNF_{300} underwent particle

deformation and tablet surface flattening due to compression. Therefore, we speculated that each CNF increased the internal and surface strength of the tablet in a similar manner, and CNF_{300}, which has a large particle size, deformed on the tablet surface, resulting in tablets of higher surface strength than that of CNF_{100}.

Tablet Disintegration Time

Figure 10 shows the disintegration time of CNF-containing tablets. For CNF_{300}, the disintegration time increased with the amount added. Upon contact with water, a tablet composed of bulk CNF swells and significantly expands in volume (Fig. 11). It is speculated that this swelling contributes to tablet disintegration. By contrast, for CNF_{100}, the disintegration time did not change when CNF added at was ≤30%. However, an increase in disintegration time was noted at 50% addition. When CNF content is low, there are fewer contact points between CNF particles within the tablet, so each particle swells when it comes into contact with water, resulting in rapid disintegration of the tablet. On the other hand, when CNF content is high, there are many contact points between CNF particles, so it is thought that these particles are intertwined. Notably, when 50% CNF was added, it was widely dispersed throughout the tablet (Fig. 7). Therefore, the adhesion between CNF particles was considered to be more dominant than disintegration. Although the tablet itself swells significantly when it comes into contact with water, we believe that it takes time for the tablet to unravel and break apart. Therefore, regardless of the tensile strength, it is inferred that a high content of CNF slows down tablet disintegration. However, all formulations except 50% CNF_{300} disintegrated within 3 min, suggesting that CNF is a useful excipient for producing tablets with favorable strength and disintegration properties.

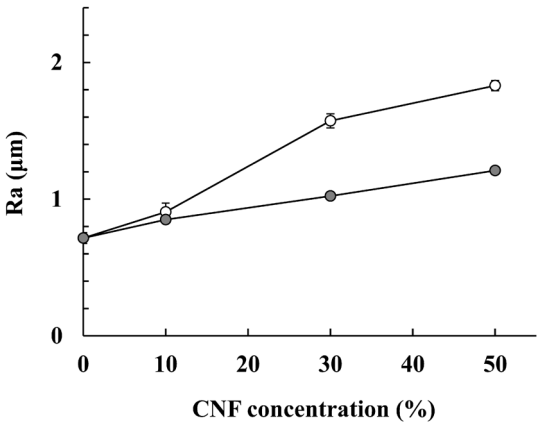

Fig. 9. Surface Roughness of Tablets Containing CNF

CNF, cellulose nanofiber; Ra, arithmetic mean roughness.

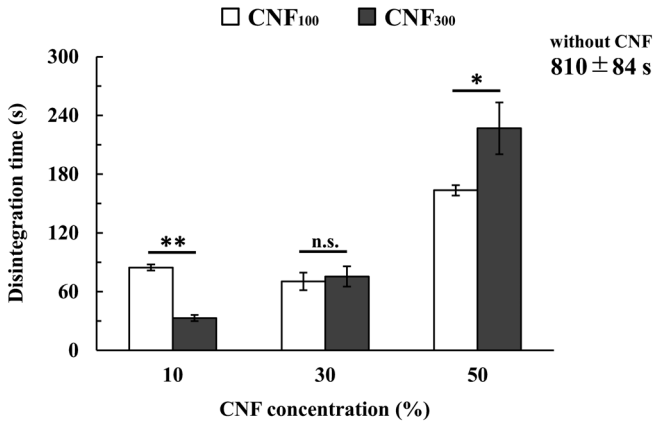

Fig. 10. Disintegration Time of CNF-Containing Tablets

The compression force during manufacture of each tablet was 10 kN. Data are presented as the mean ± S.D. ($n = 6$). Differences between tablets prepared using different additives were assessed using Student's t-test or the Mann–Whitney U test; $^{**}p < 0.001$, $^{*}p < 0.05$, n.s., not significant. CNF, cellulose nanofiber.

Drug Dissolution from Tablet

Figure 12 shows the drug dissolution behavior of each CNF-containing tablet. Table 4 also shows the similarity factor (f_2) when comparing dissolution behavior using Eq. 5. In both CNF formulations, an increase in dissolution rate was observed compared with that in tablets without CNF. In addition, when the formulations of CNF_{100} and CNF_{300} added in the same amount were compared, the dissolution rate of CNF_{300} was slower. When comparing formulations containing CNF_{100}, the drug dissolution behavior was the same regardless of the amount added ($f_2 \geq 50$). This was presumed to be attributable to the dominant effect of the solubility of the drug itself in the test medium. In the case of CNF_{300}, $f_2 < 50$ at CNF 30–50% compared with that at CNF 10%, and the drug dissolution rate decreased as the amount of CNF added increased. It was speculated that the binding force of the added CNF acted strongly, and the greater the amount added, the more difficult it was for the tablet to disintegrate, delaying the drug from coming into contact with the dissolution test medium and slowing the dissolution rate. However, the dissolution rate was higher than that of the CNF-free formulation, presumably owing to the water conductivity of added CNF. Thus, the addition of CNF to tablet formulations is expected to increase the dissolution rate of the drug. Furthermore, we considered the relationship between drug dissolution and tablet disintegration. In the case of CNF_{300}, the tablet did not completely break apart following disintegration, with CNF existing as aggregates incorporated in the drug. Therefore, we believe that drug dissolution from the aggregates changes depending on the amount of CNF added. By contrast, because the particle size of CNF_{100} is small, it does not form large aggregates like CNF_{300}, thus showing the same drug dissolution curve despite

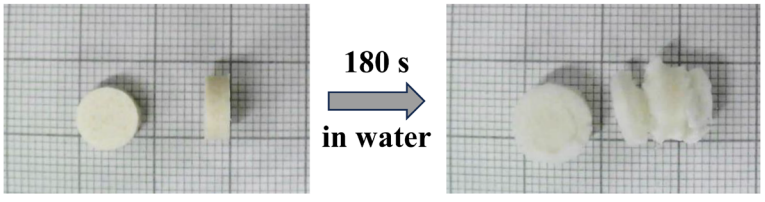

Fig. 11. Shape Changes Owing to Water Absorption by Tablets Made of Raw CNF Powder

CNF, cellulose nanofiber.

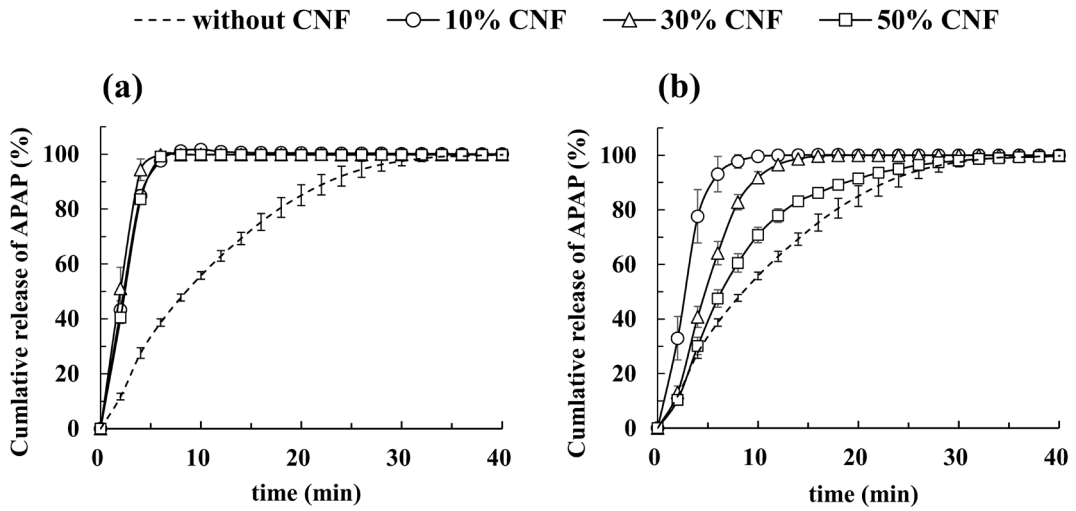

Fig. 12. Drug Dissolution from CNF-Containing Tablets

The compression force during manufacture of each tablet was 10 kN. (a) CNF_{100}-containing and (b) CNF_{300}-containing tablets. CNF, cellulose nanofiber.

Table 4. Similarity Factor (f_2) of the APAP Dissolution Profile of CNF-containing Tablets

Combination	f_2
10% CNF_{100}/30% CNF_{100}	86.68
10% CNF_{100}/50% CNF_{100}	84.73
10% CNF_{300}/30% CNF_{300}	18.99
10% CNF_{300}/50% CNF_{300}	7.63
10% CNF_{100}/10% CNF_{300}	73.89
30% CNF_{100}/30% CNF_{300}	18.62
50% CNF_{100}/50% CNF_{300}	7.37

CNF, cellulose nanofiber; f_2, similarity factor.

the amount of CNF added. To this end, it is considered that the dissolution behavior was dependent on the specific surface area of the model drug.

Conclusion

In this study, we aimed to utilize the effectiveness of CNF as a multifunctional excipient and manufacture tablets with favorable physical properties. First, even when CNF with a large particle size was pulverized, no change in crystallinity was observed. Further, it was possible to manufacture tablets *via* direct compression, regardless of CNF particle size. Evaluation of the prepared tablets revealed that the addition of CNF with a small particle size reduced the variation in tablet weight and drug content. This was attributed to the uniform dispersion of CNF in the formulation powder and the resulting friction between particles. In addition, although the effect of CNF particle size on tablet strength and disintegration was slight, addition improved both strength and disintegration. This is presumably because of the plastic deformation properties of CNF and its high affinity for water. By dispersing CNF as a fine powder inside the tablet, it was possible to produce a tablet with uniform drug content. The conventional method of manufacturing tablets by combining various excipients with specific functions has major drawbacks, such as the time required for formulation design and the high cost of excipient raw materials. Therefore, the use of CNF as a multifunctional additive may represent a highly efficient alternative. In addition, various organizations, such as the Ministry of the Environment, have pointed out the importance of developing and manufacturing products using CNF. Thus, establishing methods that utilize CNF in the pharmaceutical industry is expected to contribute toward a more sustainable society.

Experimental

Materials Lactose hydrate (Lac, diluent, Tablettose® 80, Meggle, Wasserburg, Germany), cellulose nanofiber (CNF, binder and disintegrant, ELLEX-P (alcohol-containing type), Daio Paper Corp., Tokyo, Japan), acetaminophen (APAP, model drug, Tyco Healthcare Japan, Tokyo, Japan), and magnesium stearate (Mg-St, lubricant, vegetable-based, FUJIFILM Wako Pure Chemical Corp., Osaka, Japan) were used to prepare the formulation powders. Commonly used additives, including microcrystalline cellulose (MCC; CEOLUS® KG-1000, Asahi Kasei Corp., Tokyo, Japan), low-substituted hydroxypropyl cellulose (L-HPC; LH-21; Shin-Etsu Chemical Co., Ltd., Tokyo, Japan), crospovidone (CP; Kollidon® CL, BASF, Ludwigshafen, Germany), and croscarmellose sodium (CCS; KICCOLATE™ ND-2HS, Asahi Kasei Corp.) were used as reference substances for each CNF.

CNF Pulverization CNF was pulverized using a powerful, small pulverizer (Force Mill, Osaka Chemical Co., Ltd., Osaka, Japan). Raw CNF powder (30 g) was placed in the pulverizing vessel of the apparatus. The pulverizer was temporarily stopped every 3 min and operated for a total of 18 min while stirring the powder layer with a spatula. The unpulverized CNF raw powder was denoted as CNF_{300}, and the pulverized CNF was denoted as CNF_{100}.

Evaluation of Powder Characteristics

Particle Size Distribution and Average Particle Size

The particle size distribution of each powder was measured using a laser diffraction particle size analyzer (SALD-2200, Shimadzu Corp., Kyoto, Japan) equipped with a dry measurement unit (SALD-DS5, Shimadzu Corp.), under the conditions of compressed air at 0.5 MPa and a refractive index of 1.60–0.10*i*. The D_{50} (the diameter value relative to which 50% of the particles are smaller) obtained for particle size distribution was reported as the average particle size.

Particle Shape Characterization

CNF was deposited with platinum by applying a discharge

current of 15 mA for 10 s using an ion sputtering apparatus (E-1010, Hitachi High-Tech Corp., Tokyo, Japan) set under a vacuum of 10 Pa. The shape and surface morphology of CNF particles were observed at ×50 and ×3000 using a scanning electron microscope (SEM, S-3400N, Hitachi High-Tech Corp.) in high-vacuum mode with an accelerating voltage of 5 kV. Furthermore, to evaluate the internal state of CNF in greater detail, a sample coated with an osmium plasma coater (NL-OPC80NS, Nippon Laser & Electronics Laboratory, Aichi, Japan) was observed under a field emission SEM (FE-SEM, JSM-7500F, JEOL Ltd., Tokyo, Japan) at an acceleration voltage of 3.0 kV and a magnification of approximately ×60000.

True and Tap Density

The true density was measured using a pycnometer (Ultrapyc1200e, Quantachrome, Boynton Beach, FL, U.S.A.) with helium gas. Dry powder loosely placed in a 100-mL graduated cylinder without consolidation was filled by dropping the cylinder 50 times from a height of 5 cm, and the volume of the packed powder bed was measured. The tapped density was calculated from the measured volume and weight.

Angle of Repose

The angle of repose (AOR) was measured using a powder tester (PT-S, Hosokawa Micron Corp., Osaka, Japan) in an environment of 25 ± 2 °C and 35 ± 10% relative humidity. A built-in camera photographed the powder pile formed by the free-falling formulation powder. The AOR of the formulation powder was measured directly on the acquired images using the analysis function of the instrument.

Angle of Internal Friction

Using a shear tester (NS-V100, Nanoseeds, Aichi, Japan), a shear test was performed at 25 ± 2 °C and 35 ± 10% relative humidity. A shear cell with a shear area of 14.5 cm^2 was embedded in the formulation powder, loads of 1.38×10^{-2}, 2.76×10^{-2}, and 4.14×10^{-2} MPa were applied, whereafter stress relaxation was performed. The shear stress (τ) was plotted against the vertical load (σ) on the σ–τ coordinate. The angle formed by the obtained regression line and σ axis was defined as the practical AIF.[34–37]

Compression Properties

Powder bed compression tests were performed using a tabletop tension-compression tester (MCT-2150, A&D Co., Ltd., Tokyo, Japan). A mold with a diameter of 8 mm was filled with 200 mg of pure CNF or Lac powder and compressed at a rate of 10 mm/min to evaluate the relationship between the load and the volume of the powder bed. In general, the compressibility of a powder changes depending on temporary powder properties, such as particle size, particle surface condition, and particle shape. Kawakita's equation is often used for analysis.[38–40]

$$C = \frac{V_0 - V}{V_0} = \frac{abP}{1 + bP} \tag{1}$$

where P is the vertical load, C is the volume reduction, V_0 is the initial bulk volume, V is the bulk volume under the load, a is the initial porosity, and b is the characteristic constant of the powder. Further, Eq. 1 is rewritten as follows:

$$\frac{P}{C} = \frac{1}{ab} + \frac{P}{a} \tag{2}$$

Evaluation of Wettability

A cylindrical cell with an inner diameter of 20.4 mm was filled with approximately 5 g of each CNF, which was precisely weighed, and tapped 180 times. The lower surface of the powder bed was placed on the water surface, and the distance the liquid level rose after permeating the powder bed was measured over time. These were applied to Washburn's equation (Eq. 3) to calculate the contact angle and permeation rate.[41–43]

$$\frac{l^2}{t} = \frac{r \cdot \gamma \cdot \cos\theta}{2\eta} \tag{3}$$

where, l is the permeation height of the liquid, t is the time, r is the capillary radius of the filled powder, γ is the surface tension of the liquid, η is the viscosity of the liquid, and θ is the contact angle. The permeation rate was calculated from the amount of permeated liquid 60 s after water absorption.

Water Retention

CNF (5 g) and distilled water (100 mL) were placed in a capped glass bottle, shaken well, and left for 1 d. The suspension was vacuum-filtered using a mixed cellulose ester membrane filter with a pore size of 0.45 μm (A045A047A, Advantec Toyo Kaisha, Ltd., Tokyo, Japan), followed by suction for 10 min to remove excess water. The amount of water adsorbed onto the CNF was measured after heating for 30 min using an infrared moisture meter (MB120, Ohaus, Parsippany, NJ, U.S.A.).

Crystallinity

The crystal structure of CNF was determined using a powder X-ray diffractometer (RINT ULTIMA3, Rigaku, Tokyo, Japan). A sample was placed in the apparatus, and the diffraction intensity obtained under the conditions of diffraction angle (2θ): 5–40 deg., target: Cu, tube voltage: 40 kV, and tube current: 4 mA was measured.

Preparation of Model Tablets The formulation powder for model tablet manufacture was weighed so that the total amount was 4 g; each tablet contained 20% of each CNF or common additive, and the other compositions were 74.5% Lac, 5% APAP, and 0.5% Mg-St. All materials, other than Mg-St, were mixed by shaking in a polyethylene bag for 10 min. Mg-St was then added, mixed for 5 min, and then the mixture compressed using a tabletop tableting press (HANDTAB-100, Ichihashi Seiki Co., Ltd., Kyoto, Japan) fitted with an 8 mm diameter flat-face punch to generate 200 mg tablets. The tablets of all formulations were prepared by maintaining a compression force of 10 kN for 5 s.

Preparation of the Formulation Powder The formulation powders for tablet manufacturing were mixed using a V-type mixer (DV-5, Dalton, Tokyo, Japan). Lac, CNF, and APAP at weights amounting to a total of 300 g (as shown in Table 5) were premixed for 10 min. Mg-St was then added and mixed for an additional 5 min. The resulting mixture was used as the formulation powder.

Manufacturing of Tablets *via* Continuous Tableting Direct compression was employed for the tablet manufacturing technique. Tablets were manufactured *via* continuous tableting using a rotary tableting press (VELA 5, Kikusui Seisakusho, Kyoto, Japan) equipped with a gravity feeder. A flat-face punch (8 mm-diameter) was used to compress the formulation powder with a target tablet weight of 200 mg (10 rpm, compression force: 10 kN).

Table 5. Composition of the Formulation Powder (% (w/w))

Material	F1	F2	F3	F4	F5	F6	F7
CNF_{100}	—	10	30	50	—	—	—
CNF_{300}	—	—	—	—	10	30	50
Lac	94.5	84.5	64.5	44.5	84.5	64.5	44.5
APAP	5	5	5	5	5	5	5
Mg-St	0.5	0.5	0.5	0.5	0.5	0.5	0.5

F, formulation number; CNF, cellulose nanofiber; Lac, lactose hydrate; APAP, acetaminophen; Mg-St, magnesium stearate.

Physical Properties of Tablets The physical properties of tablets were determined following storage in a desiccator for ≥1 d after tableting.

Weight Variation

Ten randomly selected tablets were weighed accurately on an electronic balance (TE214S, Sartorius, Göttingen, Germany), and the calculated coefficient of variation (% CV) was evaluated as the variation in tablet weight.

Tensile Strength

Tablet hardness was measured for 10 tablets per formulation using a hardness tester (PC-30, Okada Seiko Co., Ltd., Tokyo, Japan). Tensile strength was calculated from the hardness and the area of the tablet fracture surface using Eq. 4:

$$\text{Tensile strength (MPa)} = \frac{\text{Hardness (N)}}{\text{Tablet diameter (mm)} \times \text{Tablet thickness (mm)}} \quad (4)$$

Friability

Friability was evaluated according to the 18th Japanese Pharmacopoeia,[44] using a friability tester (TFT-120, Toyama Sangyo Co., Osaka, Japan). After brushing to remove adhering fine powder, approximately 6.5 g of the tablet was accurately weighed, placed in a friability tester, and rotated 100 times at 25 ± 1 rpm. Upon completion of the test, the recovered tablets were re-weighed after the removal of any fine powder generated during the test. Friability was calculated based on weight loss relative to the initial weight of the tablets.

Disintegration Time

Disintegration time was measured using a disintegration tester (NT-1HM, Toyama Sangyo Co.). Distilled water at 37 ± 2 °C was used as the test medium, and one tablet was placed in a glass tube inside the test basket. The disintegration time of each formulation tablet was measured six times.

Drug Content Variation

Drug content variability in tablets was determined using 10 randomly selected tablets. One tablet was stirred (IMS-1000, Tokyo Rikakikai Co., Ltd., Tokyo, Japan) for 5 min in a test tube with 10 mL of distilled water to disintegrate. It was then sonicated in an ultrasonic bath (8510J-DTH, Branson, Danbury, CT, U.S.A.) for 1 h to completely dissolve the drug. The resulting suspension was centrifuged (CF16RX II, Hitachi Koki Co., Ltd., Tokyo, Japan) at 1600 × ***g***, 20 °C for 5 min. The supernatant was filtered through a 0.45 μm syringe filter (Millex HA, Merck Millipore Corp., Darmstadt, Germany) and diluted 50-fold with distilled water. The absorbance of the diluted solution was measured using a UV spectrophotometer (U-1900, Hitachi High-Tech Corp.) set at 237.5 nm to determine the APAP weight per tablet. The APAP content was adjusted to a standardized weight of 200 mg per tablet to eliminate to the influence of tablet weight variations. The % CV of drug weight obtained was calculated and compared as the degree of drug content variation. The acceptance values were calculated according to the method described in the 18th Japanese Pharmacopoeia.[13,45]

Drug Dissolution

Dissolution of APAP from tablets to distilled water as test medium was evaluated *via* Japanese Pharmacopoeia dissolution test method 2 (paddle method). Using a flow-cell system (dissolution tester, NTR-1000, Toyama Sangyo Co.; UV-absorption photometer, U-1900, Hitachi High-Tech Corp.) with a paddle rotation speed of 50 rpm, the dissolution of APAP from one tablet over time was measured based on the absorbance at a wavelength of 237.5 nm. The cumulative release of APAP was determined by expressing the amount of APAP in the testing medium as a percentage of the defined APAP content, which was set at 100%. The similarity of dissolution profiles was evaluated using the similarity factor (f_2) calculated using the following equation:

$$f_2 = 50\log\frac{100}{\sqrt{1+\frac{\sum_{i=1}^{n}(T_i-R_i)^2}{n}}} \quad (5)$$

where n is the number of time points, while T_i and R_i are the test and reference sample amounts dissolved at each time point i, respectively. When $f_2 \geq 50$, it was determined that the two compared dissolution behaviors were equivalent.[46–48]

Distribution of CNF Particles in Tablets

Approximately 2 g of each CNF was colored by immersing it in a solution of 0.3 mg of methyl blue (Kanto Chemical Co., Inc., Tokyo, Japan) dissolved in 15 mL of distilled water for ≥24 h. The CNF collected by vacuum filtration was dried in a desiccator for ≥24 h. Dry-colored CNF was used and weighed according to the composition in Table 5, shaken in a polyethylene bag for 5 min, whereafter Mg-St was added and mixed for 2 min. The obtained formulation powder was compressed using a tabletop tableting press (HANDTAB-100, Ichihashi Seiki, Kyoto, Japan) equipped with a flat-face punch with a diameter of 8 mm under a compression force of 10 kN and a compression holding time of 5 s. A tablet prepared using colored CNF was diametrically divided into two parts to create the fracture surface of the tablet. The occupied ratio of the colored region was obtained using Image J[49,50] for the binarized image.

Statistical Analysis Statistical analysis was performed *via* the Student's *t*-test or the Mann–Whitney *U*-test using SigmaPlot 12 (Systat Software Inc., Chicago, IL, U.S.A.). Statistical significance was set at $p < 0.05$. Correlation analysis was performed using Excel Multivariate Analysis V7 (Esumi Co., Ltd., Tokyo, Japan). The correlation among factors was determined based on the coefficient of determination (R^2), where $R^2 \geq 0.49$ ($|R| \geq 0.7$) indicates strong correlation, and $0.49 > R^2 \geq 0.16$ ($0.7 > |R| \geq 0.4$) indicates moderate correlation.[51]

Acknowledgments The authors thank Daio Paper Corp. for providing the cellulose nanofiber.

Funding This research did not receive any specific grants from funding agencies in the public, commercial, or non-profit

sectors.

Conflict of Interest The authors declare no conflict of interest.

References

1) Kawashima Y., "Compression molding technology of powder," Introduction, ed. by The Society of Powder Technology, Japan: Division of Particulate Preparation and Design, Nikkan Kogyo Shimbun, Ltd., Tokyo, 1998. pp. 3–11.
2) Blanco M., Alcalá M., *Anal. Chim. Acta*, **557**, 353–359 (2006).
3) Moes J. J., Ruijken M. M., Gout E., Frijlink H. W., Ugwoke M. I., *Int. J. Pharm.*, **357**, 108–118 (2008).
4) Goodwin D. J., Van Den Ban S., Denham M., Barylski I., *Int. J. Pharm.*, **537**, 183–192 (2018).
5) Gore A. Y., McFarland D. W., Batuyios N. H., *Pharm. Technol.*, **9**, 114–122 (1985).
6) Shangraw R. F., Demarest D. A. Jr., *Pharm. Technol.*, **32**, 32–44 (1993).
7) Frake P., Greenhalgh D., Grierson S. M., Hempenstall J. M., Rudd D. R., *Int. J. Pharm.*, **151**, 75–80 (1997).
8) Sunada H., Hasegawa M., Makino T., Fujita K., Sakamoto H., Tanino T., Kawaguchi T., *J. Soc Powder Technol. Japan*, **33**, 481–486 (1996).
9) Wang X., Cui F., Yonezawa Y., Sunada H., *Chem. Pharm. Bull.*, **51**, 772–778 (2003).
10) Mahrous G. M., Shaaban D. E. Z., Shazly G. A., Auda S. H., *J. Drug Deliv. Sci. Technol.*, **39**, 192–199 (2017).
11) Sun W. J., Aburub A., Sun C. C., *J. Pharm. Sci.*, **106**, 1772–1777 (2017).
12) Yoshida I., Sakai Y., *Chem. Pharm. Bull.*, **47**, 678–683 (1999).
13) Katori N., Aoyagi N., Kojima S., *Chem. Pharm. Bull.*, **49**, 1412–1419 (2001).
14) Hara Y., *Pharm. Tech. Jpn.*, **33**, 2313–2316 (2017).
15) Katayama T., Terasawa K., Takeuchi T., Okuda Y., *Pharm. Tech. Jpn.*, **33**, 2317–2320 (2017).
16) Lukášová I., Muselík J., Franc A., Goněc R., Mika F., Vetchý D., *Eur. J. Pharm. Sci.*, **109**, 541–547 (2017).
17) Makino T., *Pharm. Tech. Jpn.*, **33**, 2309–2311 (2017).
18) Lin N., Dufresne A., *Eur. Polym. J.*, **59**, 302–325 (2014).
19) Ministry of the Environment, "Guidelines for the Utilization and Application of Cellulose Nanofiber Towards the Decarbonization and Achievement of a Circular Economy.": ‹http://www.env.go.jp/earth/earth/ondanka/cnf/guideline_summaryen.pdf›, cited 8 Augst, 2023.
20) Kargarzadeh H., Mariano M., Huang J., Lin N., Ahmad I., Dufresne A., Thomas S., *Polymer*, **132**, 368–393 (2017).
21) Sharip N. S., Ariffin H., *Mater. Today: Proc.*, **16**, 1959–1968 (2019).
22) Plackett D. V., Letchford K., Jackson J. K., Burt H. M., *Nord. Pulp. Pap. Res. J.*, **29**, 105–118 (2014).
23) Svagan A. J., Benjamins J. W., Al-Ansari Z., Shalom D. B., Müllertz A., Wågberg L., Löbmann K., *J. Control. Release*, **244** (Pt A), 74–82 (2016).
24) Bannow J., Benjamins J. W., Wohlert J., Löbmann K., Svagan A. J., *Int. J. Pharm.*, **526**, 291–299 (2017).
25) Löbmann K., Svagan A. J., *Int. J. Pharm.*, **533**, 285–297 (2017).
26) Meneguin A. B., da Silva Barud H., Sábio R. M., de Sousa P. Z., Manieri K. F., de Freitas L. A. P., Pacheco G., Alonso J. D., Chorilli M., *Carbohydr. Polym.*, **249**, 116838 (2020).
27) Liu S., Qamar S. A., Qamar M., Basharat K., Bilal M., *Int. J. Biol. Macromol.*, **181**, 275–290 (2021).
28) Raghav N., Sharma M. R., Kennedy J. F., *Carbohydr. Polym. Technol. Appl.*, **2**, 100031 (2021).
29) Nakamura S., Fukai T., Sakamoto T., *AAPS PharmSciTech*, **23**, 37 (2022).
30) Nakamura S., Nakura M., Sakamoto T., *Chem. Pharm. Bull.*, **70**, 628–636 (2022).
31) Carr R. L., *Chem. Eng.*, **18**, 163–168 (1965).
32) Nakamura S., Tanaka C., Yuasa H., Sakamoto T., *AAPS PharmSciTech*, **20**, 151 (2019).
33) Nakamura S., Nakagawa M., Tanaka C., Yuasa H., Sakamoto T., *J. Drug Deliv. Sci. Technol.*, **52**, 386–392 (2019).
34) Jenike A. W., Elsey P. J., Woolley R. H., *Proc. Am. Soc. Test Mater.*, **60**, 1168–1190 (1960).
35) Hatano S., Wang L., Shimada Y., *J. Pharmaceut. Mach. Eng.*, **19**, 62–67 (2010).
36) Japanese Standards Association: Direct shear testing method for critical state line (CSL) and wall yield locus (WYL) of powder bed. "Japanese Industrial Standard. 2016. JIS Z 8835."
37) Shimada Y., Yamamura K., Matsusaka S., *Powder Technol.*, **31**, 1007–1012 (2020).
38) Kawakita K., Lüdde K. H., *Powder Technol.*, **4**, 61–68 (1971).
39) Kawakita K., Hattori I., Kishigami M., *J. Res. Assoc. Powder Technol. Jpn.*, **8**, 453–460 (1974).
40) Denny P. J., *Powder Technol.*, **127**, 162–172 (2002).
41) Washburn E. W., *Phys. Rev.*, **17**, 273–283 (1921).
42) Szekely J., Neumann A. W., Chuang Y. K., *J. Colloid Interface Sci.*, **35**, 273–278 (1971).
43) Hamraoui A., Nylander T., *J. Colloid Interface Sci.*, **250**, 415–421 (2002).
44) Ministry of Health, Labour and Welfare. "Tablet Friability Teat," 18th ed. The Japanese Pharmacopoeia, 2021, p. 2744. ‹https://www.mhlw.go.jp/content/11120000/000904454.pdf›, cited 8 Augst, 2023.
45) Ministry of Health, Labour and Welfare. "Uniformity of Dosage Units," 18th ed. The Japanese Pharmacopoeia, 2021, pp. 161–163. ‹https://www.mhlw.go.jp/content/11120000/000945683.pdf›, cited 8 Augst, 2023.
46) Shah V. P., Tsong Y., Sathe P., Liu J. P., *Pharm. Res.*, **15**, 889–896 (1998).
47) Costa P., *Int. J. Pharm.*, **220**, 77–83 (2001).
48) Li Y. Q., Rauth A. M., Wu X. Y., *Eur. J. Pharm. Sci.*, **24**, 401–410 (2005).
49) Rasband W. S., "Image J," U.S. National Institutes of Health, Bethesda, Maryland, U.S.A., 1997–2016.
50) Schneider C. A., Rasband W. S., Eliceiri K. W., *Nat. Methods*, **9**, 671–675 (2012).
51) Guilford J. P., "Fundamental statistics in psychology and education," McGraw Hill, New York, 1956.